Journal of Medicinal Chemistry

Article

Development of Alkyne-Containing Pyrazolopyrimidines to Overcome Drug Resistance of Bcr-Abl Kinase

Chao Zhang, Alvin kung, xu liu, G. K. Surya Prakash, and Brock Malinoski

J. Med. Chem., **Just Accepted Manuscript** • DOI: 10.1021/acs.jmedchem.5b01125 • Publication Date (Web): 12 Nov 2015

Just Accepted

ACS Publications

Journal of Medicinal Chemistry is published by the American Chemical Society. 1155 Sixteenth Street N.W., Washington, DC 20036

Development of Alkyne-Containing Pyrazolopyrimidines to Overcome Drug Resistance of Bcr-Abl Kinase

Xu Liu,[†] *Alvin Kung,*[†] *Brock Malinoski,*[†] *G. K. Surya Prakash,*[†] *Chao Zhang*[*,†,‡]

[†]Loker Hydrocarbon Research Institute & Department of Chemistry, University of Southern California, University Park, Los Angeles, CA 90089, USA

[‡]USC Norris Comprehensive Cancer Center, University of Southern California, Los Angeles, CA 90089, USA

ABSTRACT:

Despite the success of imatinib at inhibiting Bcr-Abl and treating chronic myelogenous leukemia (CML), resistance to the therapy occurs over time in the patients. In particular, the resistance to imatinib caused by the gatekeeper mutation T315I in Bcr-Abl remains a challenge in the clinic. Inspired by the successful development of ponatinib to curb drug resistance, we hypothesize that the incorporation of an alkyne linker in other heterocyclic scaffolds can also achieve potent inhibition of Bcr-Abl^{T315I} by allowing for simultaneous occupancy of both the active site and the allosteric pocket in the Abl kinase domain. Herein, we describe the design, synthesis, and characterization of a series of alkyne-containing pyrazolopyrimidines as Bcr-Abl inhibitors. Our results demonstrate that some alkyne-containing pyrazolopyrimidines potently inhibit not only Abl^{T315I} *in vitro*, but also Bcr-Abl^{T315I} in cells. These pyrazolopyrimidines can serve as lead compounds for future development of novel targeted therapy to overcome drug resistance of CML.

INTRODUCTION

Chronic myelogenous leukemia (CML) is a type of cancer characterized by an uncontrolled growth of myeloid cells, a type of white blood cells.[1] Initially discovered in 1840s, CML was probably the first type of leukemia that was clearly documented.[2] It was then discovered in 1960 that the majority of CML cells harbored a reciprocal translocation between chromosome 9 and chromosome 22, which produces a short chromosome known as the Philadelphia (Ph) chromosome.[3-4] This inter-chromosomal translocation results in the fusion of two genes, breakpoint cluster region protein (BCR) and Abelson murine leukemia viral oncogene homolog 1 (ABL), normally located in chromosome 22 and 9, respectively. [1, 5]

Abl encodes a tyrosine protein kinase that is known to catalyze the transfer of phosphoryl groups to tyrosine residues in substrate proteins.[6] Cellular Abl (c-Abl) is typically located in cytoplasm and its catalytic activity is highly regulated in cells.[6] The Bcr-Abl fusion, however, is thought to induce constitutive activation of Abl activity and transform cells. Bcr-Abl has been found to be the driver of 95% chronic myelogenous leukemia (CML), and is one of the most well established oncogenes.[7] The fact that Bcr-Abl is the sole driver of most CML cases highlights the oncogenic kinase as an ideal drug target. Accordingly, pharmaceutical companies initiated programs to discover inhibitors of Bcr-Abl as CML therapy since 1990s.[8-10] Imatinib, a small-molecule inhibitor of Bcr-Abl developed by Novartis, was approved by FDA in 2001 for the treatment of CML.[11-13] This drug is the first so-called "targeted therapy" that can treat cancer by targeting a genetic lesion specific

to the cancer cells.[14] Moreover, crystal structures from the Kuriyan lab revealed that imatinib binds not only to the active site but also to a hydrophobic allosteric pocket that was only exposed upon an outward shift of the conserved DFG motif (Figure 1A).[15-16] The discovery of imatinib paves the way for the development of numerous additional type II inhibitors for a variety of protein kinases. Subsequently, some of these type II inhibitors such as sorafenib were also approved for clinical use.[17-18] The design of type II inhibitors has been rationalized for maximizing the benefits in terms of improving selectivity of protein of interest.[19-20] Imatinib utilizes a phenyl linker between the adenine pocket binder and the allosteric pocket binder (Figure 1A).[15, 21] Although the drug initially induces 67% positive therapeutic responses in CML patients, resistance is often observed within 6 months.[22-23] It has been established that the drug resistance observed in the clinic is largely due to mutations within the Abl kinase domain.[22-23] One particular mutation occurring at the gatekeeper position, T315I, accounts for approximately 20% of the resistance observed in the clinic.[24-25] This mutation was found to diminish the binding affinity of imatinib to Abl by over 100 fold due to a direct steric clash between imatinib and I315 (Figure 1B).[23, 26]

Extensive efforts were invested in the identification of novel inhibitors that can overcome imatinib-resistant mutants of Abl in the pharmaceutical industry. Out of these efforts, ponatinib was successfully developed by Ariad Pharmaceuticals to target T315I Bcr-Abl (Figure 1C).[27-29] Ponatinib contains an alkyne linker between the diarylamide side chain and the imidazo[1,2-*b*]pyridazine core.[28-29] As revealed by the crystal structure, the

slim alkyne linker is crucial to the success of ponatinib by avoiding steric clash with a bulky isoleucine residue at the gatekeeper position.[30] Nevertheless, ponatinib's sale was suspended by FDA ten months after its approval for "the risk of life-threatening blood clots and severe narrowing of blood vessels".[31] Although the suspension was partially lifted in December 2013, ponatinib prescription has to include a "Black Box Warning" and a "Risk Evaluation and Mitigation Strategy" for concerns over risks of its usage. Thus, there is still an urgent need to develop improved therapy with reduced side effects to combat CML.

We hypothesize that the introduction of an alkyne linker at proper positions on alternative heterocyclic scaffolds can also lead to compounds that inhibit T315I Bcr-Abl by avoiding steric clash with I315 (Figure 1D). We have thus designed, synthesized, and characterized a series of alkyne-containing pyrazolo[3,4-*d*]pyrimidines for the inhibition of Abl kinases. Our results show that some pyrazolopyrimidines can potently inhibit both the catalytic activity of Abl^{T315I} *in vitro*, and the activity of Bcr-Abl^{T315I} in Ba/F3 cells. Furthermore, our pyrazolopyrimidines have different kinase inhibition profiles from ponatinib. These pyrazolopyrimidines can serve as lead compounds for the development of improved therapy for overcoming drug resistance of CML.

RESULTS

We chose the pyrazolo[3,4-*d*]pyrimidine as the scaffold because it is an isosteric mimic of adenine, which can bind to the adenine-binding pocket of numerous kinases, including Abl with moderate affinity.[32-33] The C3 position of pyrazolopyrimidine was chosen to tether alkynyl substituents due to its similar position and substitution angle to the C3 position of ponatinib (Figure 1). Initially, a series of pyrazolopyrimidines **2** - **13** that contain a phenylacetylenyl group at the 3 position was synthesized. They contain diverse substituents at different positions on the phenyl ring. The synthesis exploited a common starting material, 3-iodo-1-isopropyl-1*H*-pyrazolo[3,4-*d*]pyrimidin-4-amine (**1**), which was prepared based on previously described procedures.[34] The Sonogashira coupling of **1** with various alkynes yielded **2** - **11** (Scheme 1). Treatment of **10** and **11** with BBr_3 allowed for the removal of the methyl group to give the corresponding phenol compounds **12** and **13**. The Heck coupling of 3-vinylphenol with **1** yielded **14** that contains an alkene linker instead of alkyne (Scheme 1).

After the synthesis of pyrazolopyrimidines **2** – **14**, their inhibitory activity against Abl^{WT} and Abl^{T315I} was evaluated using the phosphocellulose paper disk assay *in vitro*.[35] Imatinib and ponatinib were included in the assay as controls. As shown in Table 1, imatinib potently inhibited the enzymatic activity of Abl^{WT} (IC_{50} = 170 nM), whereas its inhibition of Abl^{T315I} was rather poor (IC_{50} = 74 μM). This translates into over 300-fold increase in the IC_{50} value of imatinib due to the T315I mutation, which is in agreement with previous reports.[23, 26] In contrast, ponatinib potently inhibited both Abl^{WT} and Abl^{T315I} with low

nanomolar IC_{50} values (Table 1). Most of the alkyne-containing pyrazolopyrimidines **2** - **13** inhibited Abl^{WT} and Abl^{T315I} with similar potency. While the alkene-containing analog **14** inhibits Abl^{WT} potently, its inhibition of Abl^{T315I} is ~5 fold less potent. These results are consistent with our hypothesis that an alkyne linker can avoid steric clash with an isoleucine residue at the gatekeeper position in Abl. Among **2** - **14**, the most effective inhibitor of Abl^{T315I} is **3**, which contains a *meta*-hydroxyl group on the phenyl ring. **3** inhibits Abl^{WT} and Abl^{T315I} with equal potency (IC_{50} = 8 nM). Nonetheless, its potency is lower than that of ponatinib. Noticing **3** and ponatinib are type I and type II inhibitors, respectively, we reasoned that the higher potency of ponatinib may stem from its additional binding to the allosteric pocket in Abl. We thus attached a 3-trifluoromethylphenyl group, a well-established binder of the allosteric pocket, via an amide linker (in forward or reverse orientation) to the *meta* position of the phenyl ring (Scheme 1).[19] The resulting **15** and **16** inhibited both Abl^{WT} and Abl^{T315I} potently, with IC_{50} values less than 2 nM (Table 1). Such potency is comparable to that of ponatinib (Table 1). These results suggest that the conversion of the alkyne-containing pyrazolopyrimidines from type I inhibitors to type II improved potency presumably due to additional binding to the allosteric pocket.

Having demonstrated potent inhibition of Abl by the alkyne-containing pyrazolopyrimidines *in vitro*, we subsequently examined their inhibition of Bcr-Abl activity in cells. Ba/F3 cells transformed with Bcr-Abl are routinely used to determine inhibition of Bcr-Abl activity in cells because their growth is dependent on the oncogenic Abl activity in the absence of the cytokine interleukin 3.[36] Similar to the *in vitro* results,

imatinib inhibits the growth of Bcr-Abl^{WT} cells at high nanomolar concentrations but not that of the T315I mutant. In comparison, ponatinib inhibits both forms with high potency (Table 2). Despite their potency spanning three orders of magnitude, our alkyne-containing pyrazolopyrimidines inhibited Bcr-Abl^{WT} and Bcr-Abl^{T315I} cells with similar potency (Figure 2). These results suggest that the alkyne linker enable potent inhibition of Bcr-Abl^{T315I} in cells by alleviating steric clash with the bulky gatekeeper residue. Among these pyrazolopyrimidines, **15** and **16** afforded the most potent growth inhibition of Ba/F3 cells expressing Bcr-Abl, demonstrating the superior potency of these two type II inhibitors in cells (Figure 2). To confirm that the observed anti-proliferative effects are due to inhibition of Bcr-Abl rather than other cellular targets, we conducted a counter-screen of the two most potent pyrazolopyrimidines against parental Ba/F3 cells that do not express Bcr-Abl. **15** and **16** do not inhibit the proliferation of parental Ba/F3 cells at concentrations below 1 μM (Table S1, Supporting Information). The over 100-fold window between IC_{50} values against parental Ba/F3 cells and those expressing Bcr-Abl suggests that anti-proliferative effects of these two pyrazolopyrimidines are due to on-target inhibition of Bcr-Abl.

In addition to examining the effects of our pyrazolopyrimidines on viability of Ba/F3 cells expressing Bcr-Abl, we investigated their effects on phospho-signal transduction in cells. Specifically, four most potent pyrazolopyrimidines (**3**, **14**, **15** & **16**) were selected along with imatinib and ponatinib and evaluated for their effects on phosphorylation of Bcr-Abl and STAT5 (Figure 3).[37-40] Since Bcr-Abl activity has been established to lead to

phosphorylation of Abl at Tyr412 and a downstream transcription factor STAT5 at Tyr694, phosphorylation levels at these sites are routinely used as markers of Bcr-Abl activity in cells. Immuno-blots with anti-pAbl and anti-pSTAT5 revealed that **15** and **16** at a concentration of 500 nM abolished phosphorylation of Abl and STAT5 in a similar manner to ponatinib in both Bcr-Abl^{WT} and Bcr-Abl^{T315I} Ba/F3 cells (Figure 3). In contrast, **3** and **14** only partially inhibited the phosphorylation of Abl and STAT5 at 500 nM, reflecting their lower potency at inhibiting Bcr-Abl in cells (Figure 3). There is little effect of the inhibitors on the total protein levels of Abl or STAT5, consistent with the notion that they exert effects through inhibiting phosphorylation rather than changing protein stability. To evaluate the potency of **15** and **16** on Bcr-Abl^{WT} and Bcr-Abl^{T315I} in cells, we determined their EC_{50} by Western blot analysis. **15** and **16** potently and effectively suppress the autophosphorylation of Bcr-Abl^{WT} (1 nM and 3 nM, respectively) and Bcr-Abl^{T315I} (20 nM and 25 nM, respectively) in a dose-dependent manner (Figure 4).

To understand the binding mode of the alkyne-containing pyrazolopyrimidines, we conducted *in silico* docking. The two most potent Abl inhibitors, **15** and **16**, were individually docked into Abl^{T315I} using AutoDock Vina. The docking models suggest that **15** and **16** can occupy the allosteric pocket and are thus type II inhibitors (Figure 5). Furthermore, these models indicate no steric clash between the bulky gatekeeper residue I315 and the alkyne linker in the pyrazolopyrimidine, which is in good agreement with the potent inhibition against Abl^{T315I} that we observed.

We determined the kinase inhibition profiles of **15**, **16** and ponatinib using the SelectScreen Kinase Profiling Services offered by Life Technologies. A diverse set of 66 kinases was selected to include common oncogenic mutants of Abl and to cover main kinase subfamilies (Table S2, Supporting Information). The profiling data show that ponatinib inhibited more kinases than **15** and **16** when all drugs were used at the same concentration of 50 nM. Despite the apparent potency difference between **15** and ponatinib, these two inhibitors share many targets in common. For example, 8 out of the 9 kinases potently inhibited (defined as >80% inhibition at 50 nM) by **15** are also potently inhibited by ponatinib. Furthermore, **15** affords moderate inhibition (40-80% inhibition) of many of the additional kinases that are potently inhibited by ponatinib, such as CSF1R and Yes1. Beyond the shared targets, ponatinib and **15** inhibited a few kinases with distinct potency. For example, Blk, MUSK and TrkA are potently inhibited by ponatinib but not significantly affected by **15**. The two pyrazolopyrimidine isomers **15** and **16** share very similar inhibition profiles to each other although the latter is generally less potent. These results suggest that the direction of the amide linker, the only structural difference between these two pyrazolopyrimidines, alters inhibitor potency but not inhibition profiles.

We had the pharmacokinetic (PK) parameters of our most potent Bcr-Abl inhibitor **15** determined at the Shanghai Medicilon Inc. Plasma levels of **15** in male SD rats were monitored after a single intravenous (IV) administration of the drug at the dose of 2 mg/kg (Figure S1, Supporting Information). The key PK parameters of **15** were summarized in Table 3. The half-life ($t_{1/2}$) of **15** was calculated to be about 1.1 h.

Discussions

In this study, we developed novel pyrazolopyrimidine-based inhibitors to overcome drug resistance caused by the T315I mutation in the Bcr-Abl kinase. An alkyne linker was featured in our inhibitor design to avoid steric clash with the isoleucine gatekeeper residue in Bcr-Abl^{T315I}. The comparable potency of these alkyne-containing pyrazolopyrimidines against Bcr-Abl^{WT} and Bcr-Abl^{T315I} suggests that the slim alkyne linker has fulfilled our design goal. Our best pyrazolopyrimidines are a few fold less potent than ponatinib at inhibiting Bcr-Abl^{T315I} in cells, which may be due to their suboptimal solubility and cell membrane permeability. Further chemical elaboration, such as installing the methyl group on the phenyl ring near the alkyne linker and the piperazine group at the end of the hydrophobic moiety, will likely improve the efficacy as well as selectivity at inhibiting Bcr-Abl in cells.

Our profiling results show that the pyrazolopyrimidine **15** shares a number of kinase targets with ponatinib. Beyond these common targets, a few kinases including Blk, MUSK and TrkA are potently inhibited by ponatinib but not significantly affected by **15**. This suggests that changing the heterocycle which occupies the adenine-binding pocket can alter kinase inhibition profile. Whether this difference in inhibition profiles can translate into better therapeutic effects remains to be tested. While the PK parameters of **15** is not excellent, it is likely that these parameters can be improved through further chemical modifications, such as installing groups to block drug metabolism or to enhance solubility.

Although structurally similar alkyne-containing pyrazolopyrimidines were recently reported, those pyrazolopyrimidines were only characterized for their inhibition of Src, an experimental drug target in triple negative breast cancer.[41] Our data show that these pyrazolopyrimidines inhibit not only Abl and Src but also a number of other kinases. It will be interesting to see if the poly-pharmacology feature of these alkyne-containing pyrazolopyrimidines can be exploited in disease settings such as CML. In another study, the imidazopyridazine core of ponatinib was replaced with a pyrazolopyridine ring to yield a small molecule GZD824 that potently inhibits Bcr-Abl^{T315I}.[26] While the pyrazolopyridine is an isostere of the pyrozolopyrimidine, the position of alkyne substitution differs between our study and theirs. The alkyne substituent was attached to the 5 position of the pyrazolopyridine in GZD824 instead of the 3 position of the pyrazolopyrimidine that we focus on here. In addition, modification beyond swapping the core with the pyrazolopyridine was not attempted at all in the study reporting GZD824.[26] Together with these prior studies, our study strongly supports the notion that the use of an alkyne linker can be a general strategy for developing inhibitors of protein kinases containing a bulky gatekeeper residue. Specifically, our study raises the interesting possibility that modifying the additional known scaffolds targeting Bcr-Abl, such as recently developed dasatinib, bosutinib and tozasertib, with an alkyne linker can lead to potent inhibitors of Bcr-Abl^{T315I}. This study is currently ongoing in our laboratory.

EXPERIMENTAL SECTION

Chemistry. ^{1}H NMR spectra were acquired on a 400 MHz Varian spectrometer and ^{13}C NMR spectra were acquired on a 500 MHz Varian spectrometer. High-resolution mass was determined using Synapt G2-Si ESI/LC-MS. All the target molecules (**2** – **16**) were found to be >95% pure based on HPLC analysis (see pages 24-31 of Supporting Information).

3-Iodo-1-isopropyl-1*H*-pyrazolo[3,4-*d*]pyrimidin-4-amine (1) was synthesized based on a known procedure.[34]

General Procedure for the cross coupling reaction between 3-iodo-1-isopropyl-1*H*-pyrazolo[3,4-*d*]pyrimidin-4-amine (**1**) and alkyne. Solid components including **1** (0.33 mmol), tetrakis(triphenylphosphine)palladium (0.066 mmol), CuI (0.165 mmol) were first added to flask (50 mL). This was followed by addition of anhydrous THF (10 mL), selected alkyne (1.32 mmol), and diisopropylamine (3.3 mmol). The reaction flask was covered by aluminum foil and the mixture was stirred for 17 h at room temperature. The reaction mixture was concentrated at reduced pressure and the crude product was purified by flash column chromatography (Hexanes/ethyl acetate).

1-Isopropyl-3-(phenylethynyl)-1*H*-pyrazolo[3,4-*d*]pyrimidin-4-amine (2). This compound was synthesized using ethynylbenzene (yield = 73%). ^{1}H NMR (400 MHz, DMSO) δ 8.25 (s, 1H), 7.75 - 7.71 (m, 2H), 7.48 - 7.45 (m, 3H), 5.04 (sep, 1H), 1.47 (d, J = 8Hz, 6H). ^{13}C NMR (125 MHz, DMSO) δ 157.60, 156.04, 152.09, 131.66, 129.23, 128.49,

124.85, 121.21, 92.76, 81.05, 48.58, 21.57 ppm. HRMS (ESI) calculated for $C_{16}H_{16}N_5$ [M+H]+ is 278.1406, found 278.1407.

3-((4-Amino-1-isopropyl-1*H*-pyrazolo[3,4-*d*]pyrimidin-3-yl)ethynyl)phenol (3). This compound was synthesized using 3-ethynylphenol (yield = 68%). ^{1}H NMR (400 MHz, DMSO) δ 9.76 (s, 1H), 8.24 (s, 1H), 7.26 (t, J = 6 Hz, 1H), 7.14 (d, J = 4 Hz, 1H), 7.07 (s, 1H), 6.88 (d, J = 4 Hz, 1H), 5.04 (sep, 1H), 1.47 (d, J = 4 Hz, 6H). ^{13}C NMR (125 MHz, DMSO) δ 157.56, 157.07, 155.99, 152.01, 129.61, 124.82, 122.41, 121.95, 117.94, 116.71, 100.46, 92.92, 80.41, 48.53, 21.51 ppm. HRMS (ESI) calculated for $C_{16}H_{16}N_5O$ [M+H]+ is 294.1355, found 294.1355.

3-((3-Aminophenyl)ethynyl)-1-isopropyl-1*H*-pyrazolo[3,4-*d*]pyrimidin-4-amine (4). This compound was synthesized using 3-ethynylaniline (yield = 66%). ^{1}H NMR (400 MHz, DMSO) δ 8.24 (s, 1H), 7.09 (t, J = 6Hz, 1H), 6.83 (s, 1H), 6.825 (d, J = 4Hz, 1H), 6.655 (d, J = 4Hz, 1H), 5.30 (s, 2H), 5.03 (sep, 1H), 1.47 (d, J = 4 Hz, 6H). ^{13}C NMR (125 MHz, DMSO) δ 157.82, 156.20, 152.19, 148.82, 129.22, 125.22, 121.42, 119.16, 116.32, 115.25, 100.68, 94.09, 79.87, 48.73, 21.74 ppm. HRMS (ESI) calculated for $C_{16}H_{17}N_6$ [M+H]+ is 293.1515, found 293.1511.

3-((3-Fluorophenyl)ethynyl)-1-isopropyl-1*H*-pyrazolo[3,4-*d*]pyrimidin-4-amine (5). This compound was synthesized using 1-ethynyl-3-fluorobenzene (yield = 50%). ^{1}H NMR (400 MHz, DMSO) δ 8.25 (s, 1H), 7.70 - 7.30 (m, 4H), 5.04 (sep, 1H), 1.47 (d, J = 6.8 Hz, 6H). ^{13}C NMR (125 MHz, DMSO) δ 162.55, 160.60, 157.48, 156.04, 152.12,

130.53, 128.04, 124.42, 123.23, 118.22, 116.37, 100.46, 91.25, 81.88, 21.53 ppm. HRMS (ESI) calculated for $C_{16}H_{15}FN_5$ [M+H]+ is 296.1311, found 296.1315.

3-((3-Chlorophenyl)ethynyl)-1-isopropyl-1*H*-pyrazolo[3,4-*d*]pyrimidin-4-amine (6). This compound was synthesized using 1-chloro-3-ethynylbenzene (yield = 75%). ^{1}H NMR (400 MHz, DMSO) δ 8.24 (s, 1H), 7.91 (t, J = 2, 1H), 7.69 (dt, J = 7.6, 1.3 Hz, 1H), 7.56 - 7.46 (m, 2H), 5.04 (sep, 1H), 1.47 (d, J = 6.8 Hz, 6H). ^{13}C NMR (125 MHz, DMSO) δ 157.45, 156.00, 152,09, 132.97, 131.10, 130.31, 130.25, 129.17, 124.38, 123.22, 100.44, 91.01, 82.17, 48.58, 21.50 ppm. HRMS (ESI) calculated for $C_{16}H_{15}ClN_5$ [M+H]+ is 312.1016, found 312.1012.

1-Isopropyl-3-(*m*-tolylethynyl)-1*H*-pyrazolo[3,4-*d*]pyrimidin-4-amine (7). This compound was synthesized using 1-ethynyl-3-methylbenzene (yield = 70%). ^{1}H NMR (400 MHz, DMSO) δ 8.25 (s, 1H), 7.57 (s, 1H), 7.52 (d, J = 7.6 Hz, 1H), 7.35 (t, J = 7.6 Hz, 1H), 7.29 (d, J = 7.6 Hz, 1H), 5.04 (sep, 1H), 2.35 (s, 3H), 1.47 (d, J = 6.8 Hz, 6H). ^{13}C NMR (125 MHz, DMSO) δ 157.57, 156.01, 152.06, 137.82, 131.98, 129.97, 128.73, 128.38, 124.86, 121.02, 100.45, 92.92, 80.75, 48.54, 21.55, 20.56 ppm. HRMS (ESI) calculated for $C_{17}H_{18}N_5$ [M+H]+ is 292.1562, found 292.1560.

1-Isopropyl-3-((3-(trifluoromethyl)phenyl)ethynyl)-1*H*-pyrazolo[3,4-*d*]pyrimidin-4-amine (8). This compound was synthesized using 1-ethynyl-3-(trifluoromethyl)benzene (yield = 45%). ^{1}H NMR (400 MHz, DMSO) δ 8.25 (s, 1H), 8.19 (s, 1H), 8.03 (d, J = 8 Hz, 1H), 7.826 (d, J = 8 Hz, 1H), 7.70 (t, J = 8 Hz, 1H), 5.05 (sep, 1H), 1.47 (d, J = 6.8 Hz, 6H). ^{13}C NMR (125 MHz, DMSO) δ 157.22, 155.80, 151.91, 135.31, 129.35, 128.07, 128.04,

125.32, 124.10, 122.24, 100.21, 90.66, 82.25, 54.47, 48.38, 21.29 ppm. HRMS (ESI) calculated for $C_{17}H_{15}F_3N_5$ [M+H]+ is 346.1280, found 346.1271.

1-Isopropyl-3-((3-methoxyphenyl)ethynyl)-1*H*-pyrazolo[3,4-*d*]pyrimidin-4-amine (9). This compound was synthesized using 1-ethynyl-3-methoxybenzene (yield = 75%). ^{1}H NMR (400 MHz, DMSO) δ 8.24 (s, 1H), 7.38 - 7.26 (m, 3H), 7.05 - 7.01 (m, 1H), 5.04 (sep, 1H), 3.81 (s, 3H), 1.47 (d, J = 8Hz, 6H). ^{13}C NMR (125 MHz, DMSO) δ 160.35, 158.96, 157.44, 153.50, 131.06, 126.18, 125.46, 123.64, 117.88, 117.10, 101.85, 94.07, 82.27, 56.57, 49.98, 22.97 ppm. HRMS (ESI) calculated for $C_{17}H_{18}N_5O$ [M+H]+ is 308.1511, found 308.1509.

1-Isopropyl-3-((4-methoxyphenyl)ethynyl)-1*H*-pyrazolo[3,4-*d*]pyrimidin-4-amine (10). This compound was synthesized using 1-ethynyl-4-methoxybenzene (yield = 54%). ^{1}H NMR (400 MHz, DMSO) δ 8.34 (s, 1H), 7.53 (d, J = 8.8Hz, 2H), 6.92 (d, J = 9.2 Hz, 2H), 6.22 (s, 2H), 5.15(sep, 1H), 3.85 (s, 3H), 1.59 (d, 6H). ^{13}C NMR (125 MHz, DMSO) δ 161.56, 157.87, 155.41, 153.00, 134.38, 127.68, 115.27, 114.30, 109.99, 95.59, 80.40, 56.36, 50.61, 22.95 ppm. HRMS (ESI) calculated for $C_{17}H_{18}N_5O$ [M+H]+ is 308.1511, found 308.1505.

1-Isopropyl-3-((2-methoxyphenyl)ethynyl)-1*H*-pyrazolo[3,4-*d*]pyrimidin-4-amine (11). This compound was synthesized using 1-ethynyl-4-methoxybenzene (yield = 46%). ^{1}H NMR (400 MHz, DMSO) δ 8.26 (s, 1H), 7.59 (dd, J = 7.6, 1.2 Hz, 1H), 7.47 (td, J = 8.8, 1.6 Hz, 1H), 7.17 (d, J = 8.0 Hz, 1H), 7.05 (td, J = 7.2, 0.8 Hz, 1H), 5.02 (sep, 1H), 3.94 (s, 3H), 1.47 (d, J = 6.8 Hz, 6H). ^{13}C NMR (125 MHz, DMSO) δ 159.92, 157.66, 156.31,

152.00, 131.86, 131.04, 124.99, 120.75, 111.22, 109.72, 101.18, 90.88, 85.49, 55.62, 48.57, 21.58 ppm. HRMS (ESI) calculated for $C_{17}H_{18}N_5O$ [M+H]+ is 308.1511, found 308.1509.

4-((4-Amino-1-isopropyl-1*H*-pyrazolo[3,4-*d*]pyrimidin-3-yl)ethynyl)phenol (12). To a stirred solution of **10** (40 mg, 0.13 mmol) in 1 mL of dry dichloromethane was added at -78 °C a solution of 1M BBr_3 in dichloromethane (0.39 mL, 0.39 mmol). After 2 h the mixture was warmed to 25 °C. The reaction was monitored by TLC; after completion, the mixture was quenched with saturated sodium bicarbonate, extracted by EtOAc, washed with water and brine. The crude product was purified by flash column chromatography (DCM/MeOH) to give a white solid (26.7 mg, 0.09 mmol, 70%). ^{1}H NMR (400 MHz, DMSO) δ 10.02 (s, 1H), 8.22 (s, 1H), 7.54 (d, J = 8.8 Hz, 2H), 6.83 (d, J = 8.4 Hz, 2H), 5.02 (sep, 1H), 1.46 (d, J = 6.4 Hz, 6H) ^{13}C NMR (125 MHz, DMSO) δ 158.63, 157.78, 156.14, 152.16, 133.56, 125.53, 115.67, 111.39, 100.48, 93.76, 79.41, 48.60, 21.73 ppm. HRMS (ESI) calculated for $C_{16}H_{16}N_5O$ [M+H]+ is 294.1355, found 294.1355.

2-((4-Amino-1-isopropyl-1*H*-pyrazolo[3,4-*d*]pyrimidin-3-yl)ethynyl)phenol (13). To a stirred solution of **11** (40 mg, 0.13 mmol) in 1 mL of dry dichloromethane was added at -78 °C a solution of 1M BBr_3 in dichloromethane (0.39 mL, 0.39 mmol). After 2 h the reaction mixture was warmed to 25 °C. The progress of the reaction was monitored by TLC; after completion, the mixture was quenched with saturated sodium bicarbonate, extracted by EtOAc, washed with water and brine. The crude product was purified by flash column chromatography (DCM/MeOH) to give a white solid (23.3 mg, 0.09 mmol, 61%).

^{1}H NMR (400 MHz, DMSO) δ 10.68 (s, 1H), 8.24 (s, 1H), 7.48 (dd, J = 7.6 Hz, 1H), 7.31-7.26 (m, 1H), 6.99 (d, J = 8Hz, 1H), 6.88 (t, J = 7.6Hz, 1H), 5.02 (sep, 1H), 1.46 (d, J = 6.8 Hz, 6H) ^{13}C NMR (125 MHz, DMSO) δ 159.03, 157.77, 152.05, 131.73, 130.74, 125.31, 119.25, 115.27, 108.42, 101.00, 91.51, 84.91, 48.49, 21.61 ppm. HRMS (ESI) calculated for $C_{16}H_{16}N_5O$ [M+H]+ is 294.1355, found 294.1356.

(*E*)-3-(2-(4-Amino-1-isopropyl-1*H*-pyrazolo[3,4-*d*]pyrimidin-3-yl)vinyl)phenol (14). A mixture of 3-vinylphenol, **14a** (100 mg, 0.83 mmol, Supporting Information), 1 (252.3 mg, 0.83 mmol), triethanolamine (124.2 mg, 0.83 mmol)) and $Pd(OAc)_2$ (8.3 mg, 0.037 mmol) was stirred under nitrogen at 100 °C for 24 h. The reaction mixture was cooled to 25 °C, quenched by the addition of dil. aq. hydrochloric acid (2M, 10 mL), and extracted with ether (3 × 100 mL). The organic phases were dried with sodium sulfate, the solvents evaporated, and the crude product was purified by flash column chromatography (hexane/ethyl acetate) to give a white solid (48.2 mg, 0.16 mmol, 54%). ^{1}H NMR (400 MHz, DMSO) δ 9.40 (s, 1H), 8.15 (s, 1H), 7.58 (d, J = 16 Hz, 1H), 7.51 (s, 2H), 7.35 (d, J = 16 Hz, 1H), 7.21 - 7.15 (m, 3H), 6.74 - 6.71 (m, 1H), 5.01 (sep, 1H), 1.48 (d, J = 6.8Hz, 6H) ^{13}C NMR (125 MHz, DMSO) δ 158.09, 157.50, 155.24, 140.23, 137.85, 131.24, 129.37, 118.41, 118.35, 115.16, 113.80, 98.15, 48.16, 21.75 ppm. HRMS (ESI) calculated for $C_{16}H_{18}N_5O$ [M+H]+ is 296.1511, found 296.1507.

***N*-(3-((4-Amino-1-isopropyl-1*H*-pyrazolo[3,4-*d*]pyrimidin-3-yl)ethynyl)phenyl)-3-(trifluoromethyl)benzamide (15).** To a solution of 4 (100 mg, 0.34 mmol) in dichloromethane (2 mL) were added triethylamine (5.2 mg, 0.05 mmol) and

3-(trifluoromethyl)benzoyl chloride (70.9 mg, 0.34 mmol). The reaction mixture was stirred at room temperature overnight, then extracted with DCM. The organic layer was washed with H_2O and dried over sodium sulfate. The solvent was removed under reduced pressure. The residue was purified by flash column chromatography (hexane/ethyl acetate) to give a yellowish solid (77.9 mg, 0.167 mmol, 49%). ^{1}H NMR (400 MHz, DMSO) δ 10.61 (s, 1H), 8.25 (s, 1H), 8.32 - 7.46 (m, 8H), 5.05 (sep, 1H), 1.48 (d, J = 6.8Hz, 6H) ^{13}C NMR (125 MHz, DMSO) δ 174.58, 165.14, 158.71, 157.15, 153.20, 139.92, 136.43, 132.83, 130.76, 130.11, 130.02, 128.34, 125.82, 125.17, 124.40, 122.60, 122.50, 109.59, 101.60, 93.67, 82.13, 49.72, 22.66 ppm. HRMS (ESI) calculated for $C_{24}H_{20}F_3N_6O$ [M+H]+ is 465.1651, found 465.1643.

3-((4-Amino-1-isopropyl-1*H*-pyrazolo[3,4-*d*]pyrimidin-3-yl)ethynyl)-*N*-(3-(trifluoromethyl)phenyl)benzamide (16). Solid components were first added to flask: 1 (88 mg, 0.29 mmol), tetrakis(triphenylphosphine)palladium (67 mg, 0.058 mmol), CuI (27.6 mg, 0.145 mmol), followed by addition of anhydrous THF (10 ml), **16b** (335.5 mg, 1.16 mmol, Supporting Information) and diisopropylamine (293.45 mg, 2.9 mmol). The reaction flask was covered in foil and the mixture was stirred for 17 h at room temperature. The reaction mixture was concentrated under reduced pressure. The compound was purified by flash column chromatography (CH_2Cl_2/MeOH) to give a light yellowish solid (60.7 mg, 0.13 mmol, 45%). ^{1}H NMR (400 MHz, DMSO) δ 10.66 (s, 1H), 8.35 (s, 1H), 7.47 – 8.24 (m, 8H) 5.04 (sep, 1H), 1.45 (d, 6H) ^{13}C NMR (125 MHz, DMSO) δ 164.84, 157.60, 156.08, 152.16, 139.64, 134.81, 134.63, 130.73, 129.79, 128.83, 128.52, 124.62, 123.65, 121.58,

120.00, 119.97, 116.27, 116.24, 116.21, 91.91, 81.87, 48.63, 21.59 ppm. HRMS (ESI) calculated for $C_{24}H_{20}F_3N_6O$ [M+H]+ is 465.1651, found 465.1644.

Protein Expression and Purification. The kinase domain of human c-Abl (residues 227-515) in modified pET-N6 vector (Plexxikon) was expressed.[42] Briefly, *E. coli* BL21 (DE3) co-transformed with Abl (pET-N6) was grown at 37 °C, [30]induced with IPTG (0.5 mM) between OD_{600} of 0.6 - 0.8 units, and then grown at 18 °C overnight. The cells were harvested by centrifugation at 4,300 rpm, re-suspended in lysis buffer (50 mM Tris, 500 mM NaCl, 25 mM imidazole, 5% glycerol, pH 7.5), and lysed by sonication (Q500 Sonicator, Qsonica). After the cell lysate was centrifuged at 10,200 × g for 1 hour at 4 °C, the supernatant was incubated with Ni-NTA beads. Then the resins were washed with wash buffer 4 times before proceeding to elution of the protein with elution buffer. The wash buffer contains 20 mM Tris, 500 mM NaCl, and 25 mM imidazole at pH 7.5 while the elution buffer is identical except a higher concentration (300 mM) of imidazole. The elution fraction was collected and analyzed by SDS-PAGE gel for purity determination.

Chicken c-Src (residues 251-533) was prepared as previously described.[43-44] In brief, the protein was co-expressed with full-length YopH phosphatase in *E. coli* BL21 (DE3) cells. The protein was initially purified by Ni-NTA beads. The 6× His-tag was then removed by TEV cleavage. Protein purification was followed with anion exchange chromatography and size-exclusion chromatography. Protein in 50 mM Tris (pH 8.0), 100 mM NaCl, 5% Glycerol, 1 mM DTT was concentrated to 10 mg/mL and flash frozen for storage at −80°C.

***In vitro* Kinase Assay.** The kinase activity was measured by quantifying the amount of ^{32}P transfer from [γ-^{32}P]–ATP to the peptide substrate. The assay was carried out in 50 mM Tris (pH 8.0), 10 mM $MgCl_2$, 5.3 nM [γ-^{32}P]– ATP (PerkinElmer), 1 mg/mL BSA, 0.1 mM peptide substrate (EAIYAAPFAKKK, Genscript) along with different concentrations of inhibitors (2 - 16) at 25°C in 30 μL reaction. The kinase reaction was initiated by the addition of [γ-^{32}P]–ATP and was allowed to proceed for 30 minutes. The reaction was transferred onto phosphocellulose filter disc paper (Whatman P81/GE Healthcare), quenched with 10% aq. acetic acid, washed with 0.5% aq. phosphoric acid (3 times), and rinsed with acetone. The dried phosphocellulose filter was added scintillation fluid (BetaMax-ES, MP Biomedicals), and counted on a scintillation counter (Beckman LC6500). The data was analyzed with GraphPad Prism5 to calculate the IC_{50}.

Cells and Reagents. Ba/F3 cells expressing Bcr-Abl^{WT} and Bcr-Abl^{T315I} were obtained from Dr. Shah laboratory (UCSF, San Francisco, CA, USA). The cells were maintained in RPMI 1640 (Corning) supplemented with 10% fetal bovine serum (v/v, HyClone, ThermoScientific) and 1X penicillin, strepatmycin, glutamine (GE Healthcare) at 37°C and 5.0% CO_2 conditions. Imatinib and ponatinib were purchased from Selleckchem. Dimethyl sulfoxide (DMSO) was purchased from Sigma-Aldrich (St. Louis, MO, USA). The following antibodies: anti-Abl, anti-phospho-Abl (Y412), anti-phospho-STAT5 (Tyr694), and anti-STAT5, were purchased from Cell Signaling (Boston, MA, USA). Anti-actin was purchased from Sigma Aldrich (St. Louis, MO, USA). Anti-mouse

secondary antibody was purchased from Jackson ImmunoResearch Laboratories (West Grove, PA, USA) while anti-rabbit secondary antibody from Abcam (Cambridge).

Western Blot Analysis. Ba/F3 cells expressing Bcr-Abl were treated with vehicle (DMSO) or drug at desired concentration for 3 hours. The cells were lysed, collected, and normalized using BCA protein assay kit (Bio-Rad) before being diluted in 1x SDS loading buffer (Bio-Rad). The samples were resolved on 4-20% SDS-page gel (Bio-Rad) and then transferred onto nitrocellulose membrane (Bio-Rad). Standard immunoblotting protocols were used. Briefly, all western blots were blocked with 5% non-fat milk in TBST (10 mM Tris, 150 mM NaCl, 0.1% Tween-20, pH 8.0) for 1 hour at room temperature. The primary antibodies were diluted to appropriate concentration and incubated overnight at 4°C Subsequently the blots were then probed with horseradish peroxidase (HRP)-conjugated secondary antibodies (1:10,000) for 1 hour at room temperature and then developed using enhanced chemiluminescence (ECL, Bio-Rad) and visualized by ChemiDoc XRS+ molecular imager (Bio-Rad).

MTT Cell Proliferation Assay. Ba/F3 cells were plated into 96-well plates (2×10^4 cells/well) and incubated with imatinib, ponatinib, or a pyrazolopyrimidine at indicated concentrations for 48 h. Subsequently, the cell viability was measured by adding MTT (Calbiochem) to all wells and incubated for 1 h. Upon completion, the reaction was quenched with formazan-solubilization reagent (50% DMF (v/v), 20% SDS w/v in H_2O) and the absorbance was measured at 540 nm using SpectraFluoro Plus plate reader (Tecan)

to determine the cell viability. Each assay was performed in triplicates and the IC_{50} values were calculated using Graphpad Prism with a nonlinear regression method.

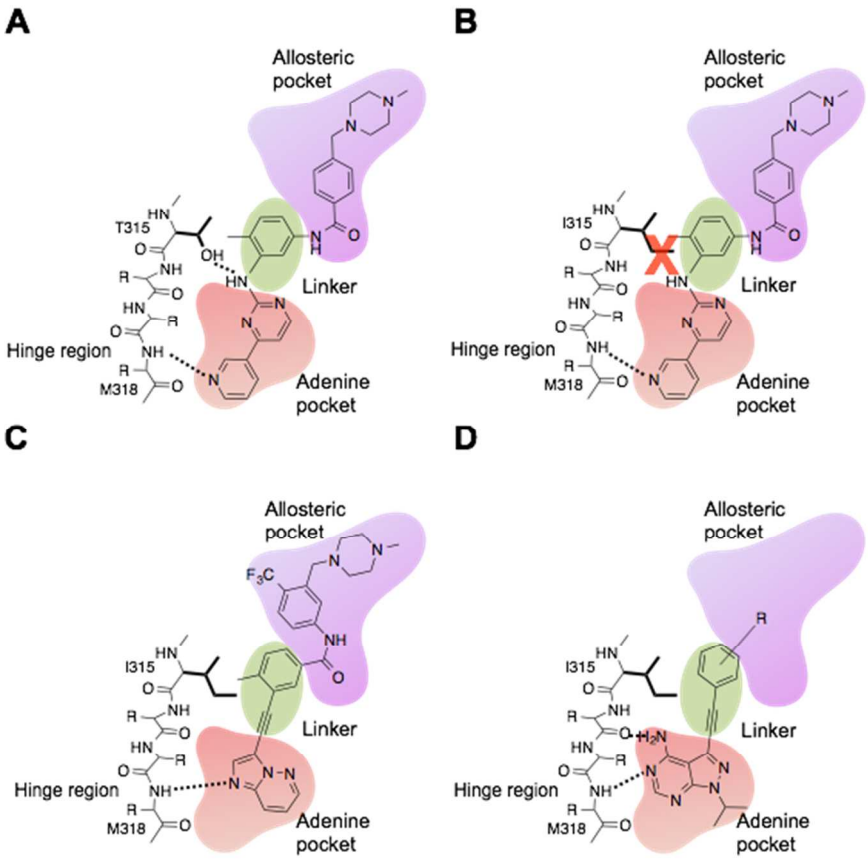

Figure 1. Schematic representations illustrating binding of the different inhibitors to the Abl kinase. (A) As a type II inhibitor, imatinib binds in both the active site and the allosteric pocket in Bcr-Abl^{WT}; (B) T315I mutation induces steric clash to imatinib and causes drug resistance; (C) an alkyne linker allows ponatinib to bypass the bulky gatekeeper residue I315 and occupy both pockets; (D) alkyne-containing pyrazolo[3,4-*d*]pyrimidines were designed to bypass I315 and bind both pockets in a similar manner to ponatinib.

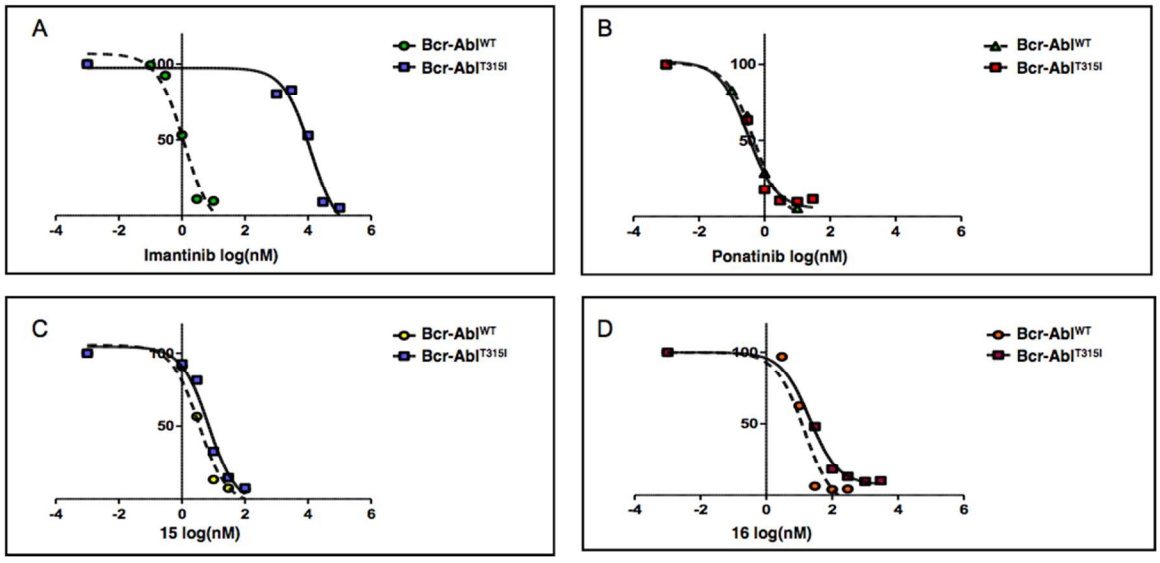

Figure 2. Effects of the inhibitors on the viability of Ba/F3 cells expressing WT or T315I Bcr-Abl. Cell viability in the presence of varying concentrations of (A) imatinib, (B) ponatinib, (C) **15**, or (D) **16** was measured using the MTT assay to generate dose-response curves (GraphPad Prism).

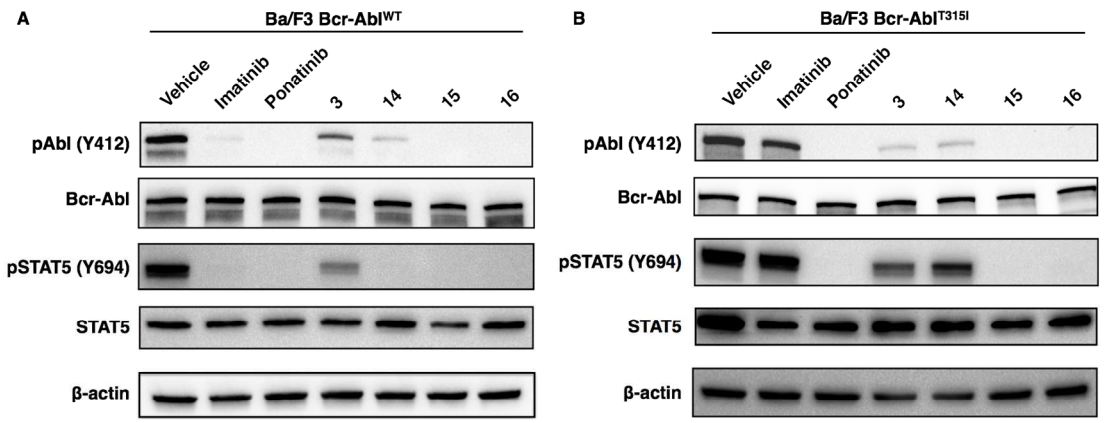

Figure 3. Pyrazolopyrimidines inhibit the activity of both (**A**) Bcr-Abl^{WT} and (**B**) Bcr-Abl^{T315I} in Ba/F3 cells as ponatinib does. Ba/F3 cells expressing Bcr-Abl^{WT} or Bcr-Abl^{T315I} were cultured at a density of 8 x 10^4/mL and treated for 3 hr at a final concentration of 500 nM for each inhibitor. The cell lysates were resolved in PAGE gel, transferred to nitrocellulose membrane, and probed with antibodies for Abl, pY412-Abl, STAT5, pY694-STAT5 and β-actin sequentially.

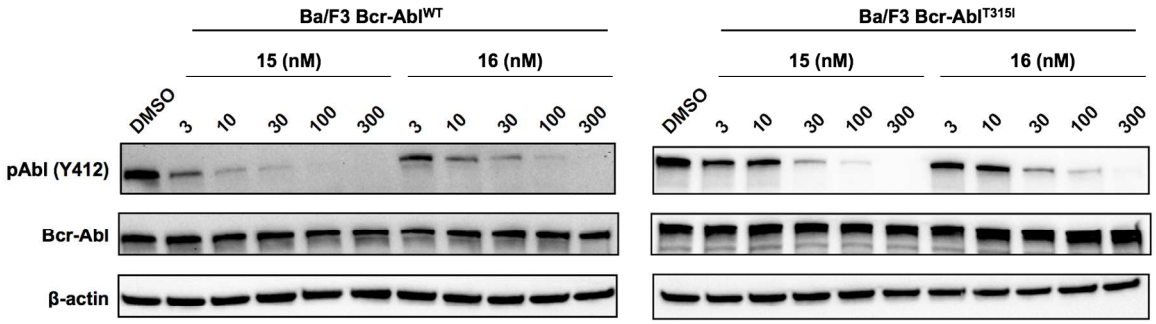

Figure 4. Pyrazolopyrimidines inhibits kinase activity of both (**A**) Bcr-Abl^{WT} and (**B**) Bcr-Abl^{T315I} in Ba/F3 cells in a dose-dependent manner. Ba/F3 cells expressing Bcr-Abl^{WT} or Bcr-Abl^{T315I} were cultured at a density of 8 x 10^4/mL and treated for 3 hr at indicated concentration for **15** and **16**. The cell lysates were resolved in PAGE gel, transferred to nitrocellulose membrane, and probed with antibodies for Abl, pY412-Abl, and β-actin sequentially.

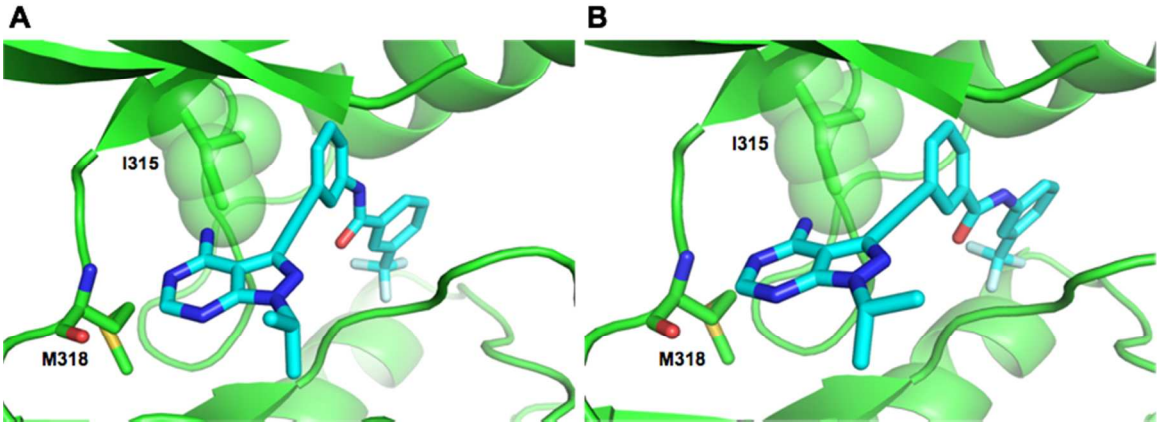

Figure 5. Docking models of Abl^{T315I} in complex with **15** (A) and **16** (B). **15** and **16** were docked into Abl^{T315I} using AutoDock Vina. A crystal structure of Abl^{T315I} in complex with a type II inhibitor (PDB entry: 3OY3) was used for docking. The images were generated using PyMol. [30]

Scheme 1. Synthesis of Pyrazolo[3,4-*d*]pyrimidines **2 - 16**

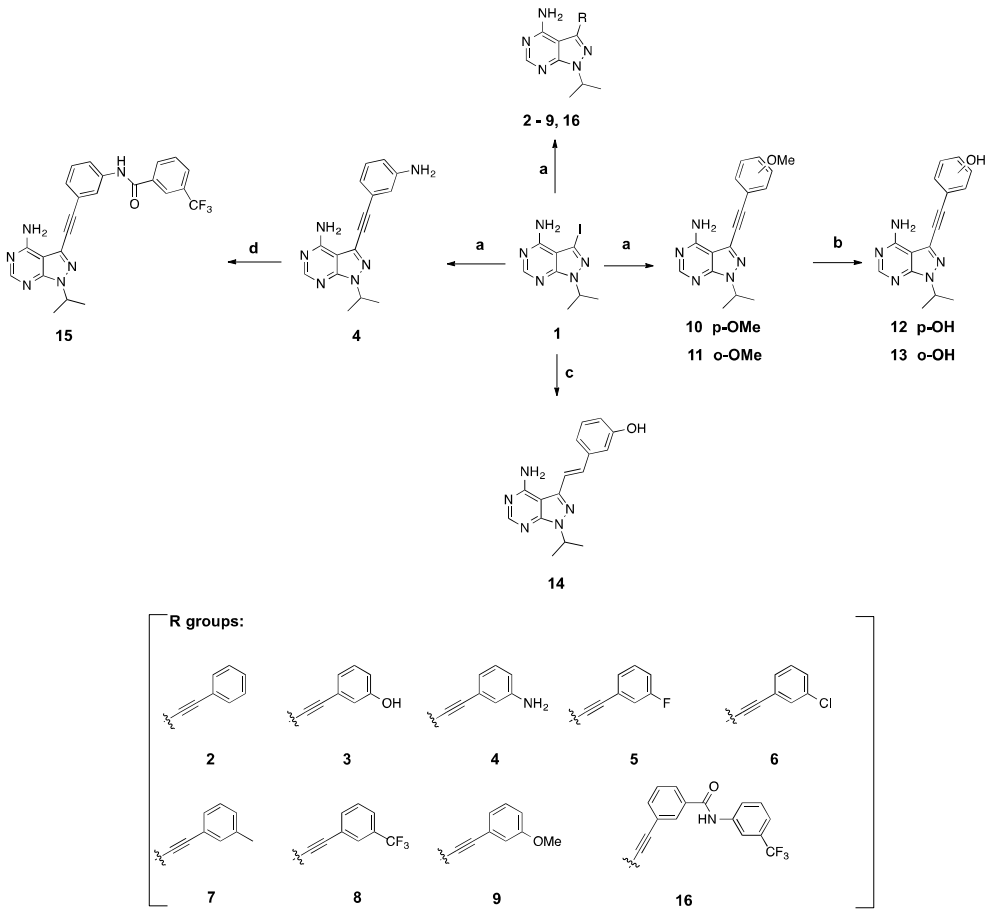

Reagents and conditions: (a) alkyne, THF, $Pd(PPh_3)_4$, CuI, N_2, r.t., 18 h; (b) BBr_3, dry DCM, -78 °C, 2 h; (c) $Pd(OAc)_2$, 3-vinylphenol, N_2, 100 °C, 24 h; (d) 3-(trifluoromethyl)benzoyl chloride, TEA, DCM, r.t., 12 h.

Table 1. Inhibitory Activity of Compounds 2 - 16 against the Abl Kinase *In Vitro*[α]

	 R	IC_{50} (nM) WT	T315I	Fold Difference
2		520	610	1.2
3	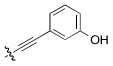	8	8	1
4	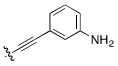	540	390	0.7
5	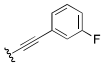	1,430	1,480	1
6	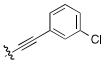	2,700	1,900	0.7
7	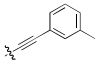	900	1,980	2.2
8	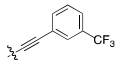	>100,000	>100,000	1
9	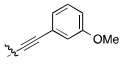	2,800	2,700	1
10	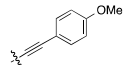	970	3,550	3.6

	 R	IC_{50} (nM) WT	T315I	Fold Difference
11		270	1,020	3.7
12	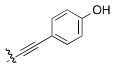	57	20	0.4
13		570	920	1.6
14		3	17	5.6
15	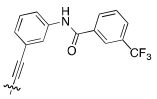	0.6	0.8	1.3
16	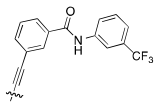	1.1	1.3	1.2
Imatinib		170	74,000	435
Ponatinib		1.4	1.6	1.1

[α]IC_{50} was determined by following the *in vitro* kinase assay protocol. The data represents the mean values of two independent experiments.

Table 2. Growth Inhibition of Ba/F3 Cells Expressing Bcr-Abl^{WT} or Bcr-Abl^{T315I} by Compounds **2** – **16**$^{\beta}$

	 R	IC_{50} (nM) WT	IC_{50} (nM) T315I	Fold Difference
2		5,020	4,500	0.9
3	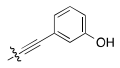	373	71	0.2
4	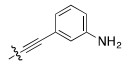	1,400	1,400	1
5	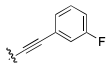	11,000	5,300	0.5
6	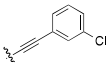	13,300	12,400	0.9
7	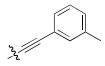	9,660	5,630	0.6
8	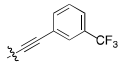	>30,000	>30,000	1
9	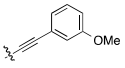	5,200	10,000	1.9
10	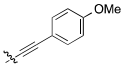	17,400	27,000	1.6
11		10,600	14,500	1.4
12	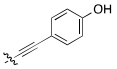	630	510	0.8
13		2,440	4,270	1.8
14		260	880	3.4
15	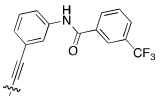	4	6	1.5
16	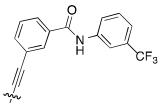	9	16	1.7
Imatinib		89	14,500	163
Ponatinib		0.4	0.3	0.8

$^{\beta}$The growth inhibition was determined using the MTT assay. Ba/F3 cells were plated in 96-well plates (2×10^4 cells/well) and incubated with the inhibitors at various concentrations for 48 h. The data represents the mean values of two independent experiments, each performed in triplicates.

Table 3. Pharmacokinetic Parameters of **15** in Rats Following IV

parameter	IV (2 mg/kg)
$AUC_{(0-\infty)}$[a] (ng/mL*h)	1708.28
$t_{1/2}$[b] (h)	1.14
C_{max}[c] (ng/mL)	1540.30
T_{max}[d](h)	0.08

[a]Mean area under the curve from the time of dosing to infinity. [b]Mean terminal half-life. [c]Mean peak plasma concentration. [d]Mean time to reach maximum plasma concentration.

ASSOCIATED CONTENT

Supporting Information

Procedures for synthesizing the intermediates and NMR spectra of the pyrazolopyrimidine products are available free of charge via the Internet at http://pubs.acs.org.

AUTHOR INFORMATION

Corresponding Author

*E-mail: zhang.chao@usc.edu. Phone: (213)-740-7040

ACKNOWLEDGMENTS

This work was supported in part by National Science Foundation (CHE-1455306), American Cancer Society (IRG-58-007-51) and the Loker Hydrocarbon Research Institute at USC. We thank N. Shah for sharing Bcr-Abl expressing Ba/F3 cells, and Plexxikon Inc. for sharing pET-SPEC-Abl plasmid construct.

References

1. Sawyers, C. L., Chronic myeloid leukemia. *New England Journal of Medicine* **1999,** *340* (17), 1330-1340.
2. Bernstein, R., Cytogenetics of Chronic Myelogenous Leukemia. *Semin Hematol* **1988,** *25* (1), 20-34.
3. Nowell, P. C.; Hungerford, D. A., Minute Chromosome in Human Chronic Granulocytic Leukemia. *Science* **1960,** *132* (3438), 1497-1497.
4. Nowell, P. C., Discovery of the Philadelphia chromosome: a personal perspective. *J Clin Invest* **2007,** *117* (8), 2033-2035.
5. Goldman, J. M.; Melo, J. V., Targeting the BCR-ABL tyrosine kinase in chronic myeloid leukemia. *New Engl J Med* **2001,** *344* (14), 1084-1086.
6. Colicelli, J., ABL Tyrosine Kinases: Evolution of Function, Regulation, and Specificity. *Sci Signal* **2010,** *3* (139).

7. Kurzrock, R.; Kantarjian, H. M.; Druker, B. J.; Talpaz, M., Philadelphia chromosome-positive leukemias: from basic mechanisms to molecular therapeutics. *Ann Intern Med* **2003,** *138* (10), 819-30.
8. Ruegg, U. T.; Burgess, G. M., Staurosporine, K-252 and Ucn-01 - Potent but Nonspecific Inhibitors of Protein-Kinases. *Trends Pharmacol Sci* **1989,** *10* (6), 218-220.
9. Zimmermann, J.; Buchdunger, E.; Mett, H.; Meyer, T.; Lydon, N. B., Potent and selective inhibitors of the Abl-kinase: Phenylamino-pyrimidine (PAP) derivatives. *Bioorg Med Chem Lett* **1997,** *7* (2), 187-192.
10. Druker, B. J.; Lydon, N. B., Lessons learned from the development of an Abl tyrosine kinase inhibitor for chronic myelogenous leukemia. *J Clin Invest* **2000,** *105* (1), 3-7.
11. Mauro, M. J.; Druker, B. J., STI571: Targeting BCR-ABL as therapy for CML. *Oncologist* **2001,** *6* (3), 233-238.
12. Capdeville, R.; Buchdunger, E.; Zimmermann, J.; Matter, A., Glivec (ST1571, Imatinib), a rationally developed, targeted anticancer drug. *Nat Rev Drug Discov* **2002,** *1* (7), 493-502.
13. Kantarjian, H.; Sawyers, C.; Hochhaus, A.; Guilhot, F.; Schiffer, C.; Gambacorti-Passerini, C.; Niederwieser, D.; Resta, D.; Capdeville, R.; Zoellner, U.; Talpaz, M.; Druker, B.; Grp, I. S. C. S., Hematologic and cytogenetic responses to imatinib mesylate in chronic myelogenous leukemia. *New Engl J Med* **2002,** *346* (9), 645-652.
14. Iqbal, N.; Iqbal, N., Imatinib: a breakthrough of targeted therapy in cancer. *Chemother Res Pract* **2014,** *2014*, 357027.
15. Schindler, T.; Bornmann, W.; Pellicena, P.; Miller, W. T.; Clarkson, B.; Kuriyan, J., Structural mechanism for STI-571 inhibition of Abelson tyrosine kinase. *Science* **2000,** *289* (5486), 1938-1942.
16. Nagar, B.; Bornmann, W. G.; Pellicena, P.; Schindler, T.; Veach, D. R.; Miller, W. T.; Clarkson, B.; Kuriyan, J., Crystal structures of the kinase domain of c-Abl in complex with the small molecule inhibitors PD173955 and imatinib (STI-571). *Cancer Res* **2002,** *62* (15), 4236-43.
17. Escudier, B., Sorafenib in advanced clear-cell renal-cell carcinoma (vol 356, pg 125, 2007). *New Engl J Med* **2007,** *357* (2), 203-203.
18. Gauthier, A.; Ho, M., Role of sorafenib in the treatment of advanced hepatocellular carcinoma: An update. *Hepatol Res* **2013,** *43* (2), 147-154.
19. Liu, Y.; Gray, N. S., Rational design of inhibitors that bind to inactive kinase conformations. *Nat Chem Biol* **2006,** *2* (7), 358-364.
20. Blanc, J.; Geney, R.; Menet, C., Type II Kinase Inhibitors: An Opportunity in Cancer for Rational Design. *Anti-Cancer Agent Me* **2013,** *13* (5), 731-747.
21. Savage, D. G.; Antman, K. H., Drug therapy: Imatinib mesylate - A new oral targeted therapy. *New Engl J Med* **2002,** *346* (9), 683-693.
22. Gorre, M. E.; Mohammed, M.; Ellwood, K.; Hsu, N.; Paquette, R.; Rao, P. N.;

Sawyers, C. L., Clinical resistance to STI-571 cancer therapy caused by BCR-ABL gene mutation or amplification. *Science* **2001,** *293* (5531), 876-80.

23. Sawyers, C. L., Research on resistance to cancer drug Gleevec. *Science* **2001,** *294* (5548), 1834.
24. O'Hare, T.; Walters, D. K.; Stoffregen, E. P.; Jia, T. P.; Manley, P. W.; Mestan, J.; Cowan-Jacob, S. W.; Lee, F. Y.; Heinrich, M. C.; Deininger, M. W. N.; Druker, B. J., In vitro activity of Bcr-Abl inhibitors AMN107 and BMS-354825 against clinically relevant imatinib-resistant Abl kinase domain mutants. *Cancer Research* **2005,** *65* (11), 4500-4505.
25. Banavath, H. N.; Sharma, O. P.; Kumar, M. S.; Baskaran, R., Identification of novel tyrosine kinase inhibitors for drug resistant T315I mutant BCR-ABL: a virtual screening and molecular dynamics simulations study. *Sci Rep-Uk* **2014,** *4*.
26. Ren, X.; Pan, X.; Zhang, Z.; Wang, D.; Lu, X.; Li, Y.; Wen, D.; Long, H.; Luo, J.; Feng, Y.; Zhuang, X.; Zhang, F.; Liu, J.; Leng, F.; Lang, X.; Bai, Y.; She, M.; Tu, Z.; Pan, J.; Ding, K., Identification of GZD824 as an orally bioavailable inhibitor that targets phosphorylated and nonphosphorylated breakpoint cluster region-Abelson (Bcr-Abl) kinase and overcomes clinically acquired mutation-induced resistance against imatinib. *J Med Chem* **2013,** *56* (3), 879-94.
27. national cancer institute FDA Approval for Ponatinib Hydrochloride. http://www.cancer.gov/about-cancer/treatment/drugs/fda-ponatinibhydrochloride (accessed 10 may).
28. O'Hare, T.; Shakespeare, W. C.; Zhu, X. T.; Eide, C. A.; Rivera, V. M.; Wang, F.; Adrian, L. T.; Zhou, T. J.; Huang, W. S.; Xu, Q. H.; Metcalf, C. A.; Tyner, J. W.; Loriaux, M. M.; Corbin, A. S.; Wardwell, S.; Ning, Y. Y.; Keats, J. A.; Wang, Y. H.; Sundaramoorthi, R.; Thomas, M.; Zhou, D.; Snodgrass, J.; Commodore, L.; Sawyer, T. K.; Dalgarno, D. C.; Deininger, M. W. N.; Druker, B. J.; Clackson, T., AP24534, a Pan-BCR-ABL Inhibitor for Chronic Myeloid Leukemia, Potently Inhibits the T315I Mutant and Overcomes Mutation-Based Resistance. *Cancer Cell* **2009,** *16* (5), 401-412.
29. Huang, W. S.; Metcalf, C. A.; Sundaramoorthi, R.; Wang, Y. H.; Zou, D.; Thomas, R. M.; Zhu, X. T.; Cai, L. S.; Wen, D.; Liu, S. Y.; Romero, J.; Qi, J. W.; Chen, I.; Banda, G.; Lentini, S. P.; Das, S.; Xu, Q. H.; Keats, J.; Wang, F.; Wardwell, S.; Ning, Y. Y.; Snodgrass, J. T.; Broudy, M. I.; Russian, K.; Zhou, T. J.; Commodore, L.; Narasimhan, N. I.; Mohemmad, Q. K.; Iuliucci, J.; Rivera, V. M.; Dalgarno, D. C.; Sawyer, T. K.; Clackson, T.; Shakespeare, W. C., Discovery of 3-[2-(Imidazo[1,2-b]pyridazin-3-yl)ethynyl]-4-methyl-N-{4-[(4-methylpiperazin-1-yl)methyl]-3-(trifluoromethyl)phenyl}benzamide (AP24534), a Potent, Orally Active Pan-Inhibitor of Breakpoint Cluster Region-Abelson (BCR-ABL) Kinase Including the T315I Gatekeeper Mutant. *J Med Chem* **2010,** *53* (12), 4701-4719.
30. Zhou, T.; Commodore, L.; Huang, W. S.; Wang, Y.; Thomas, M.; Keats, J.; Xu, Q.; Rivera, V. M.; Shakespeare, W. C.; Clackson, T.; Dalgarno, D. C.; Zhu, X., Structural

mechanism of the Pan-BCR-ABL inhibitor ponatinib (AP24534): lessons for overcoming kinase inhibitor resistance. *Chem Biol Drug Des* **2011,** *77* (1), 1-11.

31. U.S. Food and Drug administration FDA Drug Safety Communication: FDA asks manufacturer of the leukemia drug Iclusig (ponatinib) to suspend marketing and sales. http://www.fda.gov/Drugs/DrugSafety/ucm373040.htm (accessed 26 May).
32. Zhang, C.; Lopez, M. S.; Dar, A. C.; LaDow, E.; Finkbeiner, S.; Yun, C. H.; Eck, M. J.; Shokat, K. M., Structure-Guided Inhibitor Design Expands the Scope of Analog-Sensitive Kinase Technology. *Acs Chem Biol* **2013,** *8* (9), 1931-1938.
33. Liu, Y.; Bishop, A.; Witucki, L.; Kraybill, B.; Shimizu, E.; Tsien, J.; Ubersax, J.; Blethrow, J.; Morgan, D. O.; Shokat, K. M., Structural basis for selective inhibition of Src family kinases by PP1. *Chem Biol* **1999,** *6* (9), 671-8.
34. Murphy, R. C.; Ojo, K. K.; Larson, E. T.; Castellanos-Gonzalez, A.; Perera, B. G.; Keyloun, K. R.; Kim, J. E.; Bhandari, J. G.; Muller, N. R.; Verlinde, C. L.; White, A. C., Jr.; Merritt, E. A.; Van Voorhis, W. C.; Maly, D. J., Discovery of Potent and Selective Inhibitors of Calcium-Dependent Protein Kinase 1 (CDPK1) from C. parvum and T. gondii. *ACS Med Chem Lett* **2010,** *1* (7), 331-335.
35. Abukhalaf, I. K.; Masaracchia, R. A., Protein Phosphatase Assay Using a Modification of the P81 Paper Protein-Kinase Assay Procedure. *J Biochem Bioph Meth* **1993,** *26* (2-3), 95-104.
36. Wong, S.; McLaughlin, J.; Cheng, D. H.; Shannon, K.; Robb, L.; Witte, O. N., IL-3 receptor signaling is dispensable for BCR-ABL-induced myeloproliferative disease (vol 100, pg 11630, 2003). *P Natl Acad Sci USA* **2003,** *100* (26), 16143-16144.
37. Frank, D. A.; Varticovski, L., BCR/abl leads to the constitutive activation of Stat proteins, and shares an epitope with tyrosine phosphorylated Stats. *Leukemia* **1996,** *10* (11), 1724-1730.
38. Hoelbl, A.; Schuster, C.; Kovacic, B.; Zhu, B. M.; Wickre, M.; Hoelzl, M. A.; Fajmann, S.; Grebien, F.; Warsch, W.; Stengl, G.; Hennighausen, L.; Poli, V.; Beug, H.; Moriggl, R.; Sexl, V., Stat5 is indispensable for the maintenance of bcr/abl-positive leukaemia. *Embo Mol Med* **2010,** *2* (3), 98-110.
39. Shuai, K.; Halpern, J.; tenHoeve, J.; Rao, X. P.; Sawyers, C. L., Constitutive activation of STAT5 by the BCR-ABL oncogene in chronic myelogenous leukemia. *Oncogene* **1996,** *13* (2), 247-254.
40. Ye, D.; Wolff, N.; Li, L.; Zhang, S. M.; Ilaria, R. L., STAT5 signaling is required for the efficient induction and maintenance of CML in mice. *Blood* **2006,** *107* (12), 4917-4925.
41. Zhang, C. H.; Zheng, M. W.; Li, Y. P.; Lin, X. D.; Huang, M.; Zhong, L.; Li, G. B.; Zhang, R. J.; Lin, W. T.; Jiao, Y.; Wu, X. A.; Yang, J.; Xiang, R.; Chen, L. J.; Zhao, Y. L.; Cheng, W.; Wei, Y. Q.; Yang, S. Y., Design, Synthesis, and Structure-Activity Relationship Studies of 3-(Phenylethynyl)-1H-pyrazolo[3,4-d]pyrimidin-4-amine Derivatives as a New Class of Src Inhibitors with Potent Activities in Models of Triple Negative Breast Cancer. *J Med Chem* **2015,** *58* (9), 3957-74.

42. Wang, W.; Marimuthu, A.; Tsai, J.; Kumar, A.; Krupka, H. I.; Zhang, C.; Powell, B.; Suzuki, Y.; Nguyen, H.; Tabrizizad, M.; Luu, C.; West, B. L., Structural characterization of autoinhibited c-Met kinase produced by coexpression in bacteria with phosphatase. *Proc Natl Acad Sci U S A* **2006,** *103* (10), 3563-8.
43. Duan, Y. K.; Chen, L.; Chen, Y. H.; Fan, X. G., c-Src Binds to the Cancer Drug Ruxolitinib with an Active Conformation. *Plos One* **2014,** *9* (9).
44. Seeliger, M. A.; Young, M.; Henderson, M. N.; Pellicena, P.; King, D. S.; Falick, A. M.; Kuriyan, J., High yield bacterial expression of active c-Abl and c-Src tyrosine kinases. *Protein Sci* **2005,** *14* (12), 3135-9.

For Table of Contents Only